lows as many lag values as desired to be used, whilst keeping the assumed model simple.

Results from the Two-Degree-of-Freedom Example

A digitally generated two-degree-of-freedom displacement response to a frequency sweep, including noise, was analyzed using the model matching methods. The damping estimates are presented in Fig. 2 for several numbers of lags in the Correlation Fit method, and with the Least Squares Identification results obtained after decimation by two. For the scope of this note, the results are only intended to show that the Correlation Fit method works since they are only given for one sample of noise! However, indications from other work are that the Correlation Fit method is less sensitive to noise, especially where the segment includes two response peaks.

Conclusions

Two methods for rapid flutter test analysis have been examined. Both are efficient and enable modal frequency and damping estimates to be extracted from the response and excitation time histories. The Correlation Fit method is new and is presented here for the first time. It carries out a least squares fit to as many lag values of the autocorrelation and crosscorrelation functions as desired. The Least Squares Identification method is shown to be a special case of this where only a few lags are used and the fit is exact. The reason for decimation as described in Ref. 1 has been explained.

References

[1]Baird, E. F. and Clark, W. B., "Recent Development in Flight Flutter Testing in the United States," AGARD-R-596, April 1972.

[2]Waisanen, P. R. and Perangelo, H. T., "Real Time Flight Flutter Testing via Z—Transform Analysis Technique," AIAA Paper 72-784, Los Angeles, Calif., 1972.

[3]Tou, J. T., *Digital and Sampled Data Control Systems* McGraw-Hill, New York, 1959, Chap. 5.

[4]Skingle, C. W., "Correlation Techniques for Analysing the Response to a Rapid Frequency Sweep Input," *Proceedings of AIAA Symposium on Structural Dynamics and Aeroelasticity*, Boston, 1965, pp. 442–451.

[5]Lee, R. C. K., "Optimal Estimation, Identification and Control," Research Monograph 28, 1964, MIT Press, Cambridge, Mass.

Warping of Delta Wings for Minimum Drag

Rajendra K. Bera*

National Aeronautical Laboratory, Bangalore, India.

Nomenclature

AR = aspect ratio
$B(x,y)$ = complete beta function with arguments x and y
C_D = drag coefficient
C_L = lift coefficient
D = drag
e = lift dependent drag factor, $\pi AR \cdot C_D/C_L{}^2$
L = lift
$s(x)$ = local semispan
$Z(\eta)$ = ordinate distribution of mean camber surface

Received May 3, 1974; revision received July 16, 1974.
Index category: Aircraft Aerodynamics (Including Component Aerodynamics).

*Scientist, Aerodynamics Division.

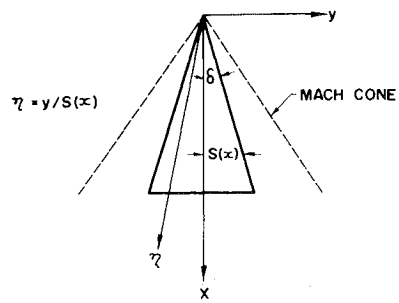

Fig. 1 Wing-Mach cone system.

α_0 = wing incidence
$\epsilon_{on}, \epsilon_n$ = constants in Eq. (1)
δ = wing semiapex angle
η = conical coordinate (Fig. 1)
λ = Lagrange multiplier

A LOW aspect ratio delta wing exhibiting an even order polynomial twist distribution was recently reported to give simple expressions for its aerodynamic and geometric properties.[1] Conical camber also has an appealing geometrical simplicity and has found successful applications in, for example, the B-58 Hustler and the Saab 37 Viggen. It was, therefore, thought worthwhile to explore the possibility of using the results of Ref. 1 to design wings of low drag subject to a given lift. This Note summarizes the results of such a study.

The delta wing is placed in a supersonic stream and is well inside the Mach cone, Fig. 1. The linearized equations permit, in such cases, solutions which have either a singularity or zero load at the leading edge. The flow at the leading edge tends to separate with the former type and hence for a smooth flow the latter type is considered by specifying the attachment line to be at the leading edge.[2,3] This produces a leading edge droop which helps alleviate drag.

We now define the nth order basic wing shape as one carrying a downwash distribution of the type

$$\omega_n(\eta) = \epsilon_{on} + \epsilon_n \eta^{2n}/2n \tag{1}$$

where η is the conical coordinate. ϵ_{on} and ϵ_n are related by the attachment condition at the leading edge through

$$\epsilon_{on} = -\frac{\epsilon_n}{2\pi n} B\left(\frac{2n+1}{2}, \frac{1}{2}\right) \tag{2}$$

where B is the complete beta function. It may be shown that the basic shapes have the property that when designed to carry a positive lift, they are at a positive incidence and have a continuous decrease of angle of attack from the wing root to the tip with the tip region showing negative values, Fig. 2a. The basic wings, therefore, will have favorable tip stall characteristics. The incidence distribution gives the mean camber surface a droop at the leading edge which becomes more pronounced with increasing n while at the same time making the central portion of the wing more flat. The surfaces are smooth and do not possess kinks, Fig. 2b.

It is now possible, using the Lagrange multiplier method, to linearly superimpose the basic shapes to obtain wings of low drag for a given lift. Physical observation may then be used to decide on the suitability of a particular design. Mathematically it means that given r basic shapes $N \equiv (n_1, n_2, \ldots, n_r)$ out of the infinite membered set given by Eq. (1) the minimum drag combination subject to a given total lift is obtained by forming the Lagrangian function

$$L \equiv C_D + \lambda C_L = \sum_{i \in N} \sum_{j \in N} C_{D_{i,j}} + \lambda \sum_{i \in N} C_{L_i} \tag{3}$$

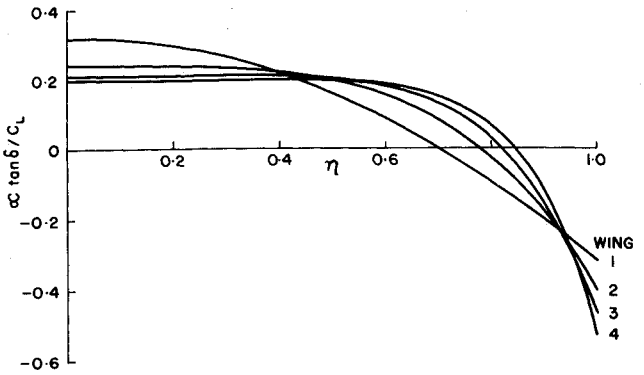

Fig. 2a Conical twist distributions (basic shapes).

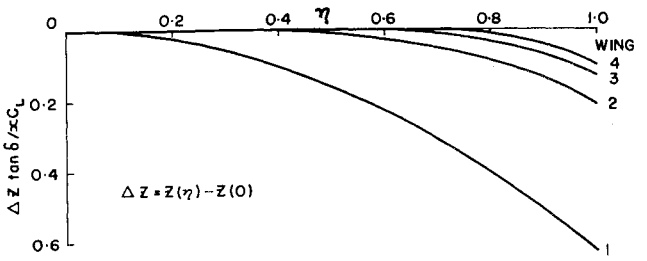

Fig. 2b Basic wing camber surfaces.

and solving the following simultaneous equations in (ϵ_i,λ) for ϵ_i.

$$\left.\begin{aligned} \partial L/\partial \epsilon_i &= 0 \qquad \text{for} \qquad i \in N \\ \partial L/\partial \lambda &= 0 \end{aligned}\right\} \tag{4}$$

Here C_D, C_L are the drag and lift coefficients, respectively, and λ is the constant Lagrange multiplier. The expressions for $C_{D(i,j)}$ and $C_{L(i)}$ as taken from Ref. 1 are (after correcting some typographical errors)

$$C_{D_{i,j}} = -\frac{\epsilon_i \epsilon_j \pi \tan\delta}{2j(2i+1)} \sum_{k=0}^{i} \frac{J_k J_{i+j-k}}{(i+j-k+1)} + \frac{\epsilon_i}{2\pi i} B\left(\frac{2i+1}{2}, \frac{1}{2}\right) C_{L_i} \tag{5}$$

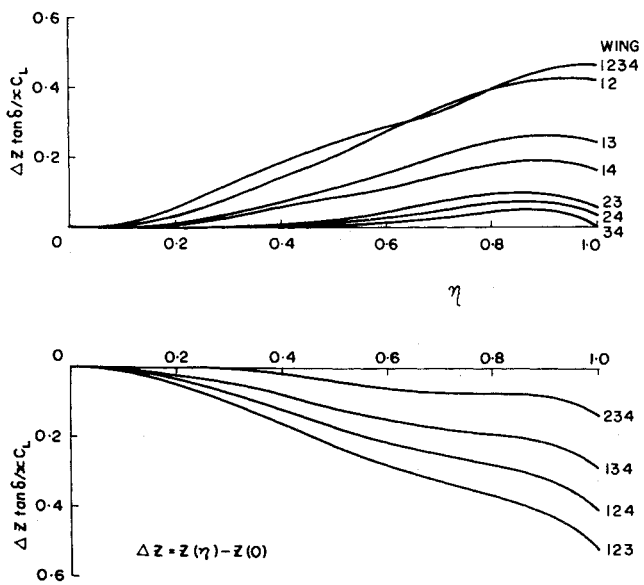

Fig. 3 Optimum wing camber surfaces.

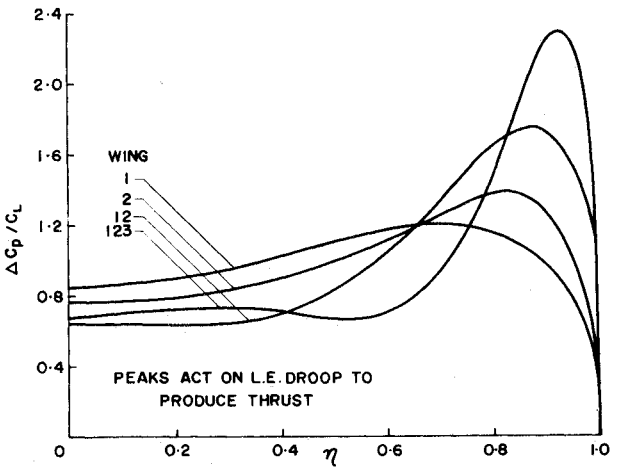

Fig. 4 Some sample spanwise pressure distributions of basic and minimum drag shapes.

$$C_{L_i} = \frac{\pi \tan\delta}{2i+1} \epsilon_i \sum_{k=0}^{i} \frac{J_k J_{i-k}}{i-k+1} \tag{6}$$

where

$$J_0 = 1, \quad J_p = \frac{1.3\ldots(2p-1)}{2.4\ldots(2p)} \tag{7}$$

The mean camber surface is then[1]

$$Z(\eta) = -x \sum_{i \in n} \left[\frac{\epsilon_i \eta^{2i}}{2i(2i-1)} + \epsilon_{0i}\right] \tag{8}$$

In this Note the first four basic shapes [n = 1,2,3,4 in Eq. (1)] are combined in all possible combinations of two, three and four and their gross aerodynamic properties are listed in Table 1. The mean camber shapes are shown in Fig. 3. Additional basic shapes in combinations of two, three and four were used but are not reported here since the trends are similar.

It is found that for even combinations, the wing ordinates lie above the η-axis, and for odd combinations, the ordinates lie below. For a given number of combinations, say a combination of three basic shapes, the wings flatten

Table 1 Gross aerodynamic properties of basic and minimum drag shapes

Wing[a]	$\frac{L}{D}\frac{C_L}{\tan\delta}$	$\frac{C_D \tan\delta}{C_L^2}$	$\frac{\alpha_0 \tan\delta}{C_L}$	$e = \pi A R C_D / C_L^2$
1	9.42	0.1061	0.318	1.3333
2	10.47	0.0955	0.239	1.2000
3	11.00	0.0909	0.212	1.1429
4	11.31	0.0884	0.199	1.1111
12	11.17	0.0895	0.119	1.1250
13	11.42	0.0875	0.133	1.1000
14	11.60	0.0862	0.139	1.0833
23	11.60	0.0853	0.146	1.0834
24	11.73	0.0849	0.149	1.0714
34	11.83	0.0845	0.152	1.0625
123	11.78	0.0849	0.212	1.0668
124	11.87	0.0843	0.204	1.0588
134	11.94	0.0838	0.196	1.0525
234	12.00	0.0833	0.186	1.0427
1234	12.08	0.0828	0.131	1.0405
Plane delta with suction	12.57	0.0796	0.159	1.0000
Plane delta without suction	6.78	0.1592	0.159	2.0000

[a] Wing 123, for example, means that basic shapes n = 1, 2, 3 are combined linearly.

out if higher order basic shapes are used. Surface waviness, apart from the leading edge droop, is small, and the number of surface waves increase with increasing number of basic shapes used in a design. All the designed shapes have a leading edge droop and a washout in incidence in the outboard portion with the tip vicinity showing negative incidences. This should, as in the basic shapes, be helpful in delaying tip stall problems.

Numerical calculations also show that combinations of higher order basic shapes or combinations of larger number of basic shapes gradually push the pressure peak outboard, increase the peak intensity, and by acting on the forward facing drooped portion of the leading edge produce a thrust force that alleviates drag, Fig. 4. Table 1 shows that the leading edge thrust lost by prescribing an attachment line at the leading edge is admirably made up by the pressures acting on the droop, and drag values quite close to the plane delta with full suction are attainable. Also, from Table 1, for even combinations, the wing incidence increases as higher order basic shapes are used. For odd combinations, the opposite trend is true.

Many of the designed shapes in Fig. 3 appear to be of practical use because of small surface waviness and favourable twist near the leading edge. In practice, the plane delta will never develop full leading edge thrust, which may be almost half the magnitude of the total drag for low aspect ratios,[5] due to flow separation. Hence, the conically cambered delta with its drooped leading edges will provide definite improvements in the lift to drag ratio in a real flow. The designs of this Note do not exhibit pronounced waviness as in Refs. 2 and 4, where the shapes were obtained by superimposing known pressure distributions, and hence our wing shapes are less conducive to produce shocks due to compressions on the wing surface.

References

[1]Bera, R. K., "The Slender Delta Wing with Conical Camber," *Journal of Aircraft*, Vol. 12, No. 4, April 1974, pp. 245–247.

[2]Smith, J. H. B. and Mangler, K. W., "The Use of Conical Camber to Produce Flow Attachment at the Leading Edge of a Delta Wing and to Minimize Lift Dependent Drag at Sonic and Supersonic Speeds," R and M 3289, 1963, Aeronautical Research Council, London.

[3]Weber, J., "Design of Warped Slender Wings with Attachment Lines Along the Leading Edge," R and M 3406, 1965, Aeronautical Research Council, London.

[4]Tsien, S. H., "The Supersonic Conical Wing of Minimum Drag," *Journal of the Aeronautical Sciences*, Vol. 22, No. 12, Dec. 1955, pp. 805–817.

[5]Jones, R. T., "Properties of Low Aspect Ratio Pointed Wings at Speeds Above and Below the Speed of Sound," Rept. 835, 1946, NACA.

Stress Diffusion in Thick Stiffened Panels

Grant P. Steven*

University of Sydney, Sydney, Australia.

Introduction

STIFFENED panels are becoming a more common structural component not only in aircraft but in civil and other transport type structures. In all applications of such structures the skin thickness between stiffeners is becoming greater and this trend makes the use of the traditional lumped stiffener[1-7] more inappropriate as will be shown herein. Finite element methods can obviously be used. However, there is always room for a closed-form solution which can illustrate more rapidly the effect of increased skin thickness in relation to the stiffener cross-sectional area.

Received December 19, 1973; revision received August 20, 1974.

Index categories: Aircraft Structural Design (Including Loads); Structural Static Analysis.

*Lecturer, Department of Aeronautical Engineering.

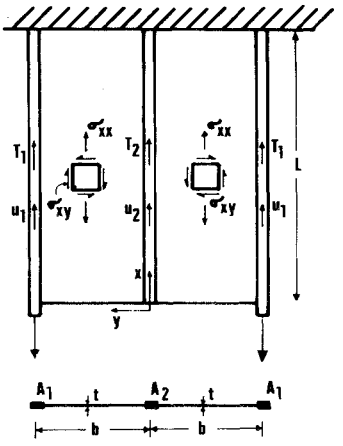

Fig. 1 Three-stringer panel showing loading and internal stress and displacement values.

In this work the skin is allowed to sustain a more natural fraction of the direct stress capacity of the panel, and its area is not lumped with the stiffeners. It can be shown that the rates at which concentrated loads diffuse into the panel are considerably altered by this technique and compare much more favorably with finite element and experimental results.

The three-stringer panel is chosen as being the simplest with which the improved stress diffusion theory can be presented. Five and seven-stringer panels have also been studied and the comments which are applied to this three-stringer panel can be applied to the others also. A sketch of the panel showing the internal stress system is given in Fig. 1. The following assumptions are made in order that the analysis can proceed. 1) The stiffeners carry only direct stress denoted by their tensions T_1 and T_2 which are functions of x. 2) The skin carries direct stress and shear stress, where the magnitude of the direct stress is constant with y and at the same level as the stress in the center unloaded stringer. This gives the correct boundary condition that direct stress be zero at the loaded end $x = 0$. 3) The panel has an infinite transverse stiffness.

On the basis of Assumption 2 and using the x-direction equilibrium equation of plane stress;

$$\partial\sigma_{xx}/\partial x + \partial\sigma_{xy}/\partial y = 0 \tag{1}$$

it can be said that since σ_{xx} is not a function of y then $\partial\sigma_{xx}/\partial x$ is not a function of y and therefore $\sigma_{xy} = -\int \partial\sigma_{xx}/\partial x \, dy$ illustrates that σ_{xy} will be a linear function of y which can be denoted as,

$$\sigma_{xy} = \tau_0 + y/b\,\tau_1 \tag{2}$$

where τ_0 and τ_1 are functions of x only. The shear strain, using Assumption 3 is;

$$\epsilon_{xy} = \frac{\partial u}{\partial y} = \frac{\sigma_{xy}}{G} \tag{3}$$

and integrating between the limits $y = 0$ and b yields

$$G(u_1 - u_2) = \tau_0 b + \tau_1 b/2 \tag{4}$$

Stress displacement relationships for the direct stresses are, using Assumption 2 for the skin;

$$T_1/A_1 = E\,du_1/dx,\ T_2/A_2 = E\,du_2/dx,$$
$$\sigma_{xx} = \sigma = E\,du_2/dx = T_2/A_2 \tag{5}$$